DETECTING EMERGENCE UNIFORMITY OF SOYBEAN SEEDLINGS ACROSS DIFFERENT CULTIVATION PATTERNS
/
不同栽培模式下大豆出苗均匀性检测

Yanxu JIAO, Jinkai QIU, Yiting LIU, Lingfeng ZHU, Hao BI, Xiuying XU*) [1]
College of Engineering, Heilongjiang Bayi Agricultural University, Daqing / China;
Tel: +86 13945925608; E-mail: xuxiuying@byau.edu.cn
Corresponding author: Xiuying Xu
DOI: https://doi.org/10.35633/inmateh-77-103

Keywords: *Soybean emergence uniformity; cultivation patterns; YOLOv12; Multiple index; Miss index*

ABSTRACT

Soybean emergence uniformity is critical for yield formation, and the early acquisition of this information provides valuable guidance for field management. However, regional variations in cultivation patterns restrict most existing detection models to a single pattern, thereby limiting their practical applicability. To overcome this limitation, this study developed a universal detection system for assessing soybean emergence uniformity across diverse cultivation patterns. The system employs unmanned aerial vehicles (UAVs) to acquire field images, after which the YOLOv12 model is used to detect seedlings and extract their center coordinates. A two-stage clustering algorithm (Elliptical DBSCAN + K-means) is applied to classify seedlings into rows, and plant spacing is calculated by integrating Euclidean distance with ground sampling distance (GSD). Emergence uniformity is subsequently evaluated using the ISO-standard Multiple and Miss Indices. Field validation across ridge-based double-row, triple-row, and quadruple-row cultivation patterns yielded coefficients of determination (R^2) of 0.9919, 0.9887, and 0.9924, respectively, with no significant differences compared to manual measurements (all $p > 0.05$). The system achieved plant-spacing detection accuracies of 96–97% during the low-occlusion VE (Vegetative Emergence) and VC (Vegetative Cotyledon) stages; however, accuracy for the quadruple-row pattern decreased to 79% at the V1 (Vegetative 1) stage due to severe leaf occlusion. This study presents the first detection framework applicable across multiple soybean cultivation patterns, providing a high-accuracy and reliable tool to support informed field management decisions.

摘要

大豆出苗均匀性是影响产量的重要因素，早期获取大豆出苗均匀性信息，可为田间管理提供指导。然而，不同地区栽培模式不同，大部分现有模型受限于一种栽培模式，存在严重局限性。为构建一种不同栽培模式下通用的大豆出苗均匀性检测系统，本研究提出一种方法，利用无人机采集大豆幼苗图像，基于 YOLOv12 模型检测幼苗并提取中心坐标；通过椭圆形 DBSCAN 和 K-means 两阶段聚类算法，将不同栽培模式下同一行大豆幼苗进行归类；结合欧几里得距离与地面采样分辨率(GSD)计算株距，并采用 ISO 标准的多重指数和缺失指数对大豆出苗均匀性进行评估。田间验证结果表明，本研究方法在垄上双行、垄上三行、垄上四行栽培模式下的株距检测决定系数 R^2 分别为 0.9919、0.9887、0.9924；均匀性指数与人工测量值无显著差异（卡方验证 P 值均 > 0.05）；系统在低遮挡的出苗期、子叶期表现优异，株距数量检测准确率高达 96%-97%，但在第一复叶时期叶面遮挡严重，垄上四行栽培模式的准确率降至 79%。本研究提出的大豆出苗均匀性检测方法首次实现了在不同栽培模式下使用，且具有较高的准确率和可靠性，可以作为田间管理决策的依据。

INTRODUCTION

Soybean seedling emergence uniformity is critical for balancing inter-plant competition for resources and serves as a key yield determinant (*Pereyra et al., 2022*). Early detection of this uniformity therefore provides vital guidance for precision field management.

[1] *Yanxu Jiao, currently pursuing a master's degree; Jinkai Qiu, currently a doctoral student; Yiting Liu, currently pursuing a master's degree; Lingfeng Zhu, currently pursuing a master's degree; Hao Bi, currently pursuing a master's degree; Xiuying Xu, Associate Professor, Doctor of Engineering.*

Conventional manual seedling counting is subjective, inefficient, and lacks full-field coverage, often leading to suboptimal management decisions (*Varela et al., 2018*). Unmanned Aerial Vehicle (UAV) remote sensing offers a flexible and low-cost solution for acquiring surface data by equipping various sensors *(Aierken et al., 2024; Gade et al., 2025*). This capability has led to its widespread integration with image processing for crop uniformity assessment in smart agriculture (*Joshi et al., 2024; Tetila et al., 2024*). Applications include evaluating uniformity in corn (*Shirzadifar et al., 2020; Vong et al., 2022*), segmenting cotton seedlings for spacing analysis (*Feng et al., 2020*), achieving crop row identification and plant segmentation *(Sunoj et al., 2025*), and assessing wheat emergence (Liu et al., 2017). However, such traditional image processing methods are prone to missegmentation under conditions of dense occlusion, which limits their accuracy.

Deep learning offers a more robust solution for agricultural image analysis, enabling effective extraction of plant information from imagery *(Valente et al., 2020)*. Notably, the YOLO series of algorithms has demonstrated high efficiency and accuracy for crop detection in complex field environments *(Kamilaris & Prenafeta-Boldú, 2018; Pham et al., 2023*). YOLO-based approaches have been successfully applied to tasks fundamental to uniformity assessment, including plant counting and geolocation, as well as to direct evaluations of spacing and uniformity *(Furlanetto et al., 2025; Liu et al., 2023; Ren et al., 2024*). Nevertheless, most research has focused on low-density crops with wide spacing. Investigations into the emergence uniformity of high-density crops like soybeans remain scarce. Furthermore, the practical application of existing models is limited by their inability to adapt to diverse regional cultivation patterns, such as the varying ridge and inter-row distances characteristic of the dominant double-row, triple-row, and quadruple-row ridge planting systems in northern China.

To address these gaps, this study developed a universal system for the rapid and accurate assessment of soybean emergence uniformity across these multiple patterns. The system integrates UAV imagery with the YOLOv12 (You Only Look Once version 12) model for seedling detection and center coordinate extraction. A two-stage clustering algorithm (Elliptical DBSCAN + K-means) classifies seedlings into rows and calculates inter-plant spacing. Finally, uniformity is evaluated using the ISO-standard Multiple and Miss Indices. By overcoming the adaptability limitations of previous models, this system provides precise field data to support scientifically informed management decisions and help ensure soybean yields.

MATERIALS AND METHODS

Experimental sites

For the double-row cultivation pattern on ridges, the inter-ridge distance was 110 cm, and the inter-row distance was 55 cm. The experimental site was at Plot 1 of the Science and Technology Park of Jianshan Farm in Heihe City, Heilongjiang Province, China. For the triple-row cultivation pattern on ridges, the inter-ridge distance was maintained at 110 cm, while the inter-row distance was set at 22.5 cm. The experimental location was Plot 9, North of Jianshan Farm in Heihe City, Heilongjiang Province, China. Regarding the quadruple-row cultivation pattern on ridges, the inter-ridge distance was 130 cm. The distance between the first and second rows, as well as between the third and fourth rows, was 10 cm, and the distance between the second and third rows was 20 cm. The experiment was conducted at the 4-4 soybean experimental field of Gongqing Farm in Jiamusi City, Heilongjiang Province, China. Across all three cultivation patterns, the seed-to-seed spacing was uniformly set at 7 cm.

Data collection

A DJI MAVIC 3M UAV equipped with a visible-light camera was used as the image acquisition platform for soybean field data collection. The visible-light camera was fitted with a 4/3 CMOS sensor, with a width of 1.74 cm, a height of 1.30 cm, and a focal length of 1.026 cm, providing an effective resolution of 20 megapixels. During data acquisition, the UAV was flown at an altitude of 5 m and captured images in a vertically downward orientation. The original image resolution was 5280 × 3956 pixels.

The Vegetative Emergence (VE), Vegetative Cotyledon (VC), and Vegetative 1 (V1) stages of soybeans were chosen for this research. The soybeans were sown in the experimental field on April 25, 2025. Image acquisition was done on sunny days with minimal wind or gentle breezes to ensure image quality. A total of 415 images were collected to construct a soybean dataset for model training. Specifically, 122 images were obtained from the double-row cultivation pattern on ridges, 156 from the triple-row pattern, and 137 from the quadruple-row pattern. Figure 1 presents the original images acquired under these three different cultivation patterns.

Double-row-on-ridge *Triple-row-on-ridge* *Quadruple-row-on-ridge*

Fig. 1 – Original images of some soybean seedlings under three cultivation patterns

To validate the model's effectiveness across different cultivation patterns, five 3.3 m × 3.3 m plots were randomly established for the ridge-based double-row pattern and five for the ridge-based triple-row pattern respectively, and five 3.9 m × 3.9 m plots for the ridge-based quadruple-row pattern. Each plot contained 3 soybean ridges, consistent with the number of ridges in the dataset-constructing images. Plot boundaries were marked with white ropes; three small green flags and one small red flag (designated as the plot's starting position) were placed at each plot's four vertices. The distance between adjacent seedlings in each plot row was measured manually, and these measurements were compared with results from the soybean emergence uniformity detection system to ultimately evaluate the model's detection accuracy.

Dataset construction

The original UAV-acquired images had a resolution of 5280×3956 pixels, whereas the input size required by YOLO algorithms is 640×640 pixels. Consequently, the original images were cropped to remove seedling-free regions, from which 4,900 images were randomly selected to form the initial dataset. However, deep learning models are prone to overfitting, which can impair generalization performance and reduce detection accuracy on unseen data. To address this issue, data augmentation was applied. As illustrated in Figure 2, 600 images were randomly selected from the cropped dataset and subjected to flipping, random 90° rotations, contrast enhancement, and brightness enhancement. These operations increased both the quantity and diversity of training samples, thereby improving model robustness.

Original image *Flip* *Random 90° rotation* *Contrast enhancement* *Brightness enhancement*

Fig. 2 – Data augmentation examples

A total of 7300 images of soybean seedlings in three growth periods were constructed through image cropping and data augmentation techniques. The images were annotated using the professional annotation tool, LabelImg. Specifically, for the VE, VC, and V1 periods, the corresponding labels were set as 0, 1, and 2, respectively. The annotated dataset was randomly partitioned into a training set, a validation set, and a test set in a ratio of 7:2:1. Such a partitioning strategy is conducive to alleviating the problems of overfitting and underfitting.

Soybean seedling recognition model

YOLOv12 model

YOLOv12 was jointly proposed by the University at Buffalo and the University of Chinese Academy of Sciences in February 2025. It utilized the attention mechanism for the first time to substitute the CNN framework as the backbone network. The aim was to tackle the problem of the traditional YOLO series overly depending on CNN while overlooking the attention mechanism (*Tian et al., 2025*). As presented in Figure 3, the network structure of YOLOv12 is elaborated as follows. The original ELAN *(Zhang et al., 2022*) was optimized in the Backbone section, and the Residual Efficient Layer Aggregation Network (R-ELAN) with enhanced stability was implemented. Additionally, a regional attention mechanism was incorporated, which enlarged the receptive field and decreased the computational complexity. Regarding the Neck part, an improved PANet (*Liu et al., 2018*) architecture was adopted. Integrating the Feature Pyramid Network and the Path Aggregation Network achieved a comprehensive fusion of features at various levels, enhancing detection

performance. In the Head component, the Anchor-Free mechanism was employed. This mechanism directly predicts the center points of objects, enabling the model to detect target objects of different sizes adaptively.

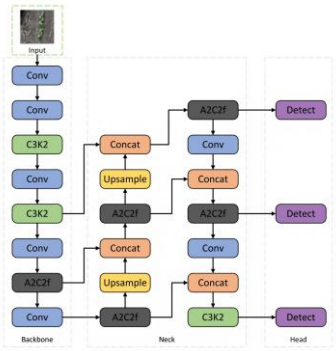

Fig. 3 – Network structure of YOLOv12

Experimental environment configuration

In this research, a PyTorch deep - learning framework was established to carry out training and testing on the annotated dataset. The operating system employed was Windows 11 (64-bit). The central processing unit (CPU) was an Intel(R) Core(TM) i7-14700HX. The graphics processing unit (GPU) was an NVIDIA GeForce RTX 4060 Laptop GPU. The random-access memory (RAM) was 16GB, and the graphics card's video memory was 8GB. The training environment was configured as follows: Python version 3.9.19, PyTorch version 2.2.0, and CUDA version 12.6. For the model training, 200 epochs were conducted, with a batch size of 8 and an initial learning rate of 0.01.

Detection of soybean emergence uniformity

Extraction of soybean seedling centers

Calculating the distance between adjacent seedlings and comparing it with the standard distance is a crucial prerequisite for evaluating the uniformity of soybean emergence. The YOLOv12 detection results output coordinates in a normalized format. However, to compute the actual distance between the centers of two seedlings, it is necessary to convert these normalized coordinates into actual pixel coordinates. By retrieving the image's original width and height information, the normalized abscissa is multiplied by the original width, and the normalized ordinate is multiplied by the original height. This enables us to obtain the actual coordinates of the soybean seedling center points in pixel units. Figure 4 illustrates the actual coordinate positions of the center points representing soybean seedlings across three cultivation patterns. The calculation formula is presented as Equation (1):

$$\begin{cases} x = x_n \cdot W \\ y = y_n \cdot H \end{cases} \quad (1)$$

where:

x, y are the actual coordinates of the seedling center point, [px]; x_n, y_n are the normalized coordinates (dimensionless); W, H are the width and height of the original image, [px].

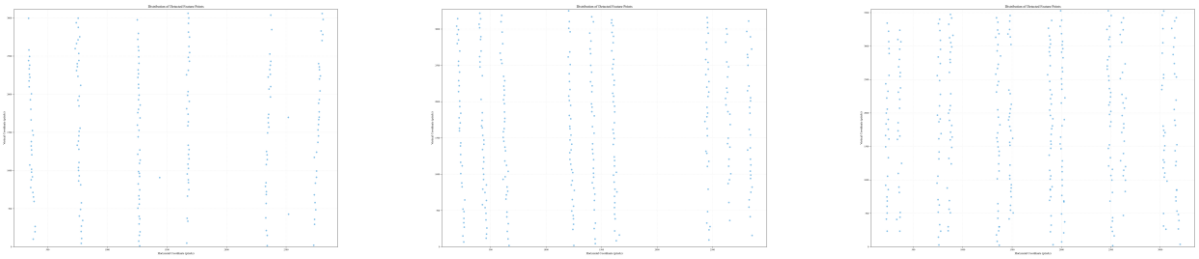

Double-row-on-ridge *Triple-row-on-ridge* *Quadruple-row-on-ridge*

Fig. 4 – Actual coordinates of soybean center points

Clustering of soybean center coordinate points

In order to compute the actual distances between the center points of adjacent soybean seedlings within a row, it is necessary to categorize the extracted center points according to the cultivation patterns. Given that there are variations in the ridge spacing, row spacing, and the number of rows on each ridge under

different cultivation patterns, directly clustering the crop rows is likely to introduce errors. Hence, in this study, a two-stage clustering approach of "first clustering by ridges and then by rows" is employed.

The experiment incorporates the elliptical DBSCAN clustering algorithm *(Li et al., 2024)*. This algorithm capitalizes on the characteristics of crops arranged in rows, the relatively consistent distance between adjacent rows, and the minimal slope variations. Even in uneven spacing within a row or missing seedlings, accurate clustering can still be achieved, thereby exhibiting strong robustness. The clustering scope is regulated by adjusting three parameters: the length of the major semi-axis a, the minor semi-axis b, and the minimum number of samples for core points N_{Minpts}. To identify the optimal parameters, the total number of points correctly clustered is utilized as the evaluation metric for screening. The optimal parameters for the three cultivation patterns are presented in Table 1. The results of ridge-based clustering are depicted in Figure 5. All points under the three cultivation patterns are accurately clustered by ridges, which provides a solid foundation for subsequent row-based clustering.

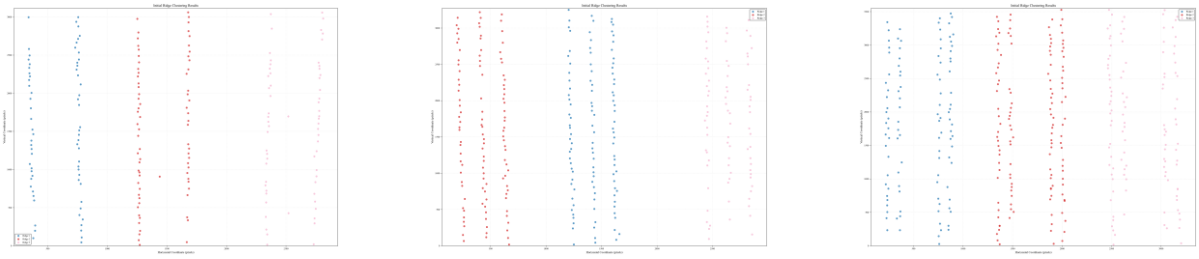

Double-row-on-ridge *Triple-row-on-ridge* *Quadruple-row-on-ridge*

Fig. 5 – Clustering effect diagram of soybean ridges

Table 1

Clustering parameters of soybean ridges under different cultivation patterns

Clustering parameters	Double-row-on-ridge	Triple-row-on-ridge	Quadruple-row-on-ridge
Semi-major axis, a [px]	1200	900	1200
Semi-minor axis, b [px]	1000	700	1100
NMinpts	5	5	5

On the basis of ridge clustering, it is necessary to further classify the seedlings within the same ridge into their respective rows. Given the differences in the number of rows per ridge and the row spacing among the three cultivation patterns, this study first pre-defined the K value according to the pattern. Specifically, K was set to 2, 3, and 4 for double-row, triple-row, and quadruple-row ridges, respectively. Subsequently, Principal Component Analysis (PCA) was employed to identify the direction of maximum data variance, which corresponds to the extension direction of the ridge. All coordinate points were then projected onto the axis perpendicular to this primary direction. Finally, the K-means algorithm was utilized to cluster the projected points, thereby accomplishing the classification of rows within the same ridge. Figure 6 presents the results of row-based clustering, showing that all points under the three cultivation patterns were accurately assigned to their respective crop rows. This result establishes a reliable foundation for calculating the spacing between adjacent plants within each row.

Double-row-on-ridge *Triple-row-on-ridge* *Quadruple-row-on-ridge*

Fig. 6 – Clustering effect diagram of soybean rows

In large-scale fields, certain seedlings may be far from soybean crop rows—for example, Figure 7(a) (ridge-based double-row cultivation) shows such seedlings in rows 3, 5, and 6. To eliminate their interference with plant spacing calculation, this study used an outlier detection method for filtering. Setting the outlier parameter to 8 pixels effectively removed redundant seedlings: as shown in Figure 7(b), the three distant

coordinate points were marked with red crosses (indicating successful removal), and all remaining points fell within the reasonable range of crop rows. This makes the calculated plant spacing more consistent with reality and ensures stable, reliable results.

(a) Before outlier removal *(b) After outlier removal*

Fig. 7 – Outlier filtering

Calculation of soybean plant spacing

The distance between adjacent soybean seedlings within the same crop row is a key indicator for evaluating soybean emergence uniformity. According to the agronomic planting practices at the experimental site, the sowing interval for soybeans was set at 7 cm. Let the coordinates of two adjacent seedlings be denoted as (x_1,y_1) and (x_2,y_2), respectively. The Euclidean distance formula was used to calculate the spacing D between adjacent seedlings. The calculation method is given in Equation (2):

$$D=\sqrt{(x_2-x_1)^2+(y_2-y_1)^2} \tag{2}$$

The distance D between adjacent centroids represents the actual pixel distance. The actual ground distance corresponding to a single pixel in the image is calculated by means of GSD_W (the ground sampling distance in the horizontal direction). The calculation method is expressed as Equation (3):

$$GSD_W=\frac{w_s \cdot h}{f \cdot n_w} \tag{3}$$

where:

GSD_W is the ground sampling distance in the horizontal direction, [cm/px]; w_s denotes the sensor width, [cm]; h represents the flight altitude, [m]; f stands for the lens focal length, [cm]; n_w refers to the number of pixels in the width direction of the image, [px].

The distances between adjacent seedlings in the image were calculated and visualized by connecting them with line segments labeled with their corresponding lengths. As shown in Figure 8, blue segments represent distances less than 0.5 times the standard soybean spacing, red segments represent distances greater than 1.5 times this spacing, and green segments represent distances within the normal range.

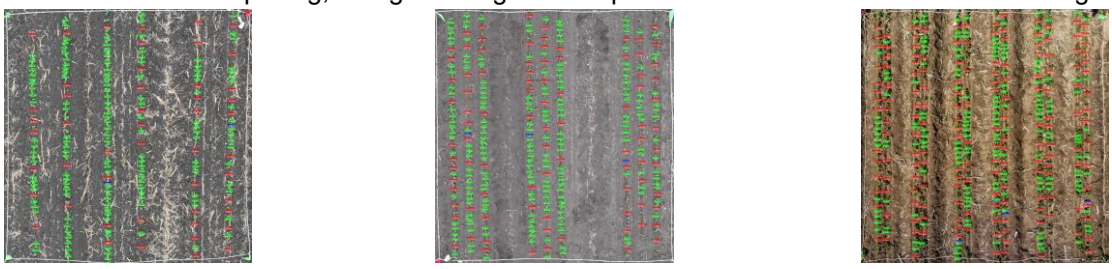

Double-row-on-ridge *Triple-row-on-ridge* *Quadruple-row-on-ridge*

Fig. 8 – Detection effect diagram of soybean plant spacing

Evaluation metrics

Evaluation metrics for the YOLOv12 model

This study evaluates the detection results using four indicators: precision, recall, F1-score, and mean average precision (mAP). The specific calculation formulas for these indicators are provided in Equations (4)—(8) (*Gao et al., 2020*).

$$Precision = \frac{TP}{TP + FP} \tag{4}$$

$$Recall = \frac{TP}{TP + FN} \quad (5)$$

$$mAP = \frac{\sum_{i=1}^{n} AP_i}{n} \quad (6)$$

$$F_1 = 2*Precision*Recall/(Precision+Recall) \quad (7)$$

$$Accuracy = (1 - \frac{|N_T - TP|}{N_T}) \times 100\% \quad (8)$$

where:

TP (True Positives) is the number of soybean seedlings correctly detected by the model; FP (False Positives) is the number of background or non-target objects incorrectly identified as seedlings; FN (False Negatives) is the number of actual soybean seedlings that were not detected by the model; AP_i (Average Precision) is the average precision for class i; n is the total number of classes; N_T is the total number of actual soybean seedlings in the plot (ground truth).

Evaluation metrics for soybean emergence uniformity

As the mean value and standard deviation among seeds are not ideal descriptors for seed spacing uniformity (*Kachman & Smith, 1995*), the ISO multiple index and ISO missing index are adopted to assess the emergence uniformity *(Singh et al., 2005)*.

The International Organization for Standardization (ISO) multiple index standard judges all spacings less than 0.5 times the theoretical spacing as multiples.

$$Multiple\ Index\% = \frac{N_1}{N_T} \times 100 \quad (9)$$

Here, N_1 represents the number of distances that are less than 0.5 times the theoretical distance. Meanwhile, “Multiple” refers to the scenario in which two or more seeds are present in a space where only one seed is expected.

By the ISO standard, any distance exceeding 1.5 times the theoretical distance is considered a case of missing seedlings. The missing-seedling rate is calculated using the following formula:

$$Miss\ Index\% = \frac{N_2}{N_T} \times 100 \quad (10)$$

Here, N_2 represents the number of distances that are greater than 1.5 times the theoretical distance. Moreover, “Miss” refers to the situation where no seeds are sown in the area where seeds are theoretically supposed to be sown.

The ISO multiple index and the ISO missing index are expressed as percentages of the theoretical inter-seed distance. A smaller value indicates better emergence uniformity.

RESULTS

Comparative experiments

Through a horizontal comparison with four mainstream object detection models, namely YOLOv5, YOLOv8, YOLOv11, and RTDETR (as presented in Table 2), YOLOv12 attains an optimal balance in the average performance of detection accuracy and speed. This accomplishment meets the dual requirements of high-quality detection and efficient computation. With an mAP@50 of 95.3% and a detection speed of 213 ms, YOLOv12 effectively ensures the reliability of uniformity detection. Consequently, in this study, YOLOv12 is chosen as the detection model for soybean seedlings.

Table 2

Comparison of the performance of different models

Model	Precision [%]	Recall [%]	mAP@50 [%]	Detection speed [%]
Yolov5	87.7	90.9	95.1	315
Yolov8	87.2	92.3	95.4	345
Yolov11	87.6	92.3	95.6	303
Yolov12	87.7	91.5	95.3	213
RTDETR	84.1	88.7	92.4	114

Accuracy verification of soybean emergence uniformity detection

Detection performance under different cultivation patterns

The YOLOv12 model was employed to detect soybean seedlings in one of the plots under various cultivation patterns. Subsequently, the number of plant-to-plant spacings within each plot of different cultivation patterns was meticulously counted. The accuracy of the model's detection is defined as the proportion of the number of adjacent seedling spacings successfully detected by the model to the total number of such spacings. Table 3 presents detailed results. As the table shows, for the double-row and triple-row cultivation patterns on the ridges, YOLOv12's accuracy in detecting the number of plant-to-plant spacings of soybean seedlings reached 97% and 96%, respectively. However, in the case of the four-row cultivation pattern on the ridges, the accuracy was merely 79%. This discrepancy can be attributed to the fact that most soybean seedlings in this plot were in the V1 growth stage. Moreover, the row spacing on the ridges was narrower than that of the double-row and triple-row cultivation patterns, measuring only 10 cm. This led to more pronounced leaf-to-leaf occlusion, resulting in a relatively large number of missed detections by the model and ultimately influencing the overall detection outcome.

Table 3

Detection Accuracy of Soybean Seedling Spacing Under Different Cultivation Patterns

Cultivation Pattern	Actual total number of plant spacing	Total number of plant spacing detected by the model	Accuracy [%]
Double-row-on-ridge	237	231	97
Triple-row-on-ridge	275	263	96
Quadruple-row-on-ridge	394	313	79

Accuracy verification of plant spacing

Plant spacing is critical for assessing soybean emergence uniformity. To validate the algorithm's plant spacing detection accuracy across cultivation patterns, this study compared its results with manual measurements and calculated the coefficient of determination. To eliminate interference from undetected plants, detected seedlings were strictly matched to actual plants; if undetected plants existed between two detected seedlings, the distance between these two seedlings was calculated and compared with the corresponding actual spacing.

The calculation results for the three cultivation patterns are presented in Figure 9. For the double-row cultivation pattern on the ridge, the coefficient of determination R^2 is 0.9919, and the slope of the trend line concerning the diagonal line y = x is 0.9622. In the case of the triple-row cultivation pattern on the ridge, the coefficient of determination R^2 is 0.9887, and the trend line slope relative to the diagonal y = x is 0.9819. Regarding the four-row cultivation pattern on the ridge, the coefficient of determination R^2 is 0.9924, and the slope of the trend line corresponding to the diagonal y = x is 0.9614. These results indicate that despite missed detections, the system still demonstrates a high level of accuracy in calculating the inter-plant distances of the detected adjacent seedlings.

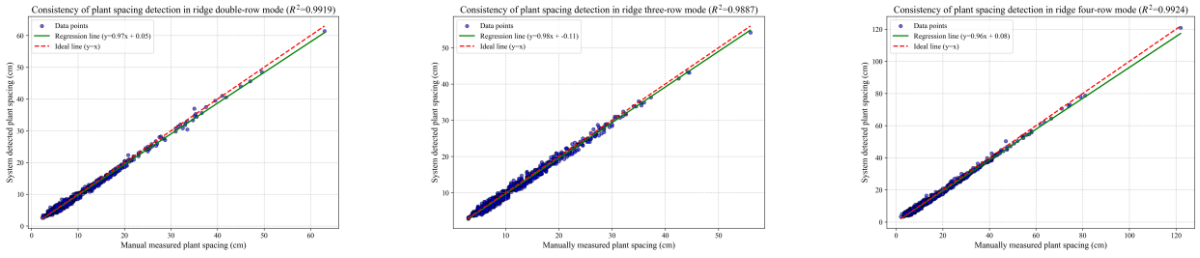

Double-row-on-ridge *Triple-row-on-ridge* *Quadruple-row-on-ridge*

Fig. 9 – Result diagram of determination coefficients under different cultivation patterns

Accuracy verification of multiple and missing detections

To evaluate the accuracy of the model in detecting multiple and miss events across different cultivation patterns, one experimental plot per pattern was selected for validation. The counts of multiple, miss, and normal plant spacing from manual measurements were compared with model-detected results, as shown in

Table 4. The misdetection counts were 8, 28, and 81 for double-row, triple-row, and quadruple-row ridge patterns, respectively. Errors increased significantly in the quadruple-row pattern, primarily because all plants were at the V1 growth stage with severe leaf occlusion. Normal spacing was misclassified as miss due to undetected intermediate seedlings, which increased the measured distance between adjacent plants. Similarly, actual multiple spacing was misjudged as normal due to missing detections, while actual miss events were amplified by undetected plants, collectively reducing detection accuracy.

Table 4

Comparison of manually counted and model-detected quantities of multiple, missed, and normal plant spacings

Cultivation pattern	Category	Actual number	Detected number	Error number
Double-row-on-ridge	Multiple plant spacing	7	2	5
	Missing plant spacing	46	47	1
	Normal plant spacing	184	182	2
Triple-row-on-ridge	Multiple plant spacing	1	0	1
	Missing plant spacing	75	83	8
	Normal plant spacing	199	180	19
Quadruple-row-on-ridge	Multiple plant spacing	11	2	9
	Missing plant spacing	118	106	12
	Normal plant spacing	265	205	60

To validate whether the detection accuracy under the three cultivation patterns can be applied in practical scenarios, a chi-square goodness-of-fit test was employed to analyze the consistency between the manually detected and system-detected values. The null hypothesis was set as: there is no significant difference between the two datasets. The results are presented in Figure 10. For the double-row cultivation pattern on the ridge, the p-value is 0.2563; for the triple-row cultivation pattern on the ridge, the p-value is 0.3515; and for the quadruple-row cultivation pattern on the ridge, the p-value is 0.0698. At a significance level of α, since the p-values of all three cultivation patterns are greater than 0.05, it indicates that there is no significant difference between the manually measured values and the system-detected values. This effectively validates the effectiveness of the model.

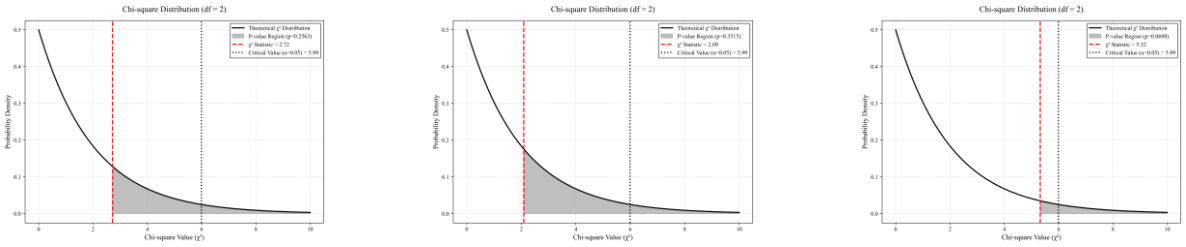

Double-row-on-ridge *Triple-row-on-ridge* *Quadruple-row-on-ridge*

Fig. 10 – Result diagram of chi-square fitting verification under different cultivation patterns

Evaluation of soybean emergence uniformity

Emergence uniformity was evaluated for each cultivation pattern using ISO-standard Multiple and Miss Indices, with results derived from Table 4. The ridge-based double-row cultivation pattern yielded a Multiple Index of 0.87%, a Miss Index of 20.35%, and an overall error of 3.02%. Corresponding values for the triple-row pattern were 0%, 27.27%, and 4.65%, and for the quadruple-row pattern, 0.64%, 33.87%, and 6.07%.

These results indicate that the ridge-based double-row cultivation pattern exhibited the highest emergence uniformity, with both indices lower than those of the triple- and quadruple-row patterns. Notably, the Miss Index was substantially higher than the Multiple Index across all patterns, suggesting that missed seeding is a greater concern than over-seeding. Subsequent field management should therefore prioritize addressing seed omission to improve emergence uniformity and promote optimal soybean growth.

CONCLUSIONS

This study developed a universal system for detecting soybean emergence uniformity across multiple cultivation patterns by integrating UAV imagery, the YOLOv12 model, and an innovative two-stage clustering algorithm. Validation confirmed the system's reliability for field management, with optimal performance during the early growth stages (VE/VC). However, performance declined at the V1 stage, primarily due to severe leaf occlusion in high-density patterns. This work provides a practical tool for precision agriculture, and future efforts will focus on enhancing robustness against occlusion and improving regional generalization.

ACKNOWLEDGEMENT

This work was supported by the Doctoral Research Startup Fund Project of Heilongjiang Bayi Agricultural University [grant number XDB202501].

REFERENCES

[1] Aierken, N., Yang, B., Li, Y., Jiang, P., Pan, G., & Li, S. (2024). A review of unmanned aerial vehicle based remote sensing and machine learning for cotton crop growth monitoring. *Computers and Electronics in Agriculture*, 227, 109601.

[2] Feng, A., Zhou, J., Vories, E., & Sudduth, K. A. (2020). Evaluation of cotton emergence using UAV-based narrow-band spectral imagery with customized image alignment and stitching algorithms. *Remote Sensing*, 12(11), 1764.

[3] Furlanetto, R. H., Boyd, N. S., & Buzanini, A. C. (2025). Multi-Crop Plant Counting and Geolocation Using a YOLO-Powered GUI System. *Smart Agricultural Technology*, 100994.

[4] Gade, S. A., Madolli, M. J., García-Caparrós, P., Ullah, H., Cha-um, S., Datta, A., & Himanshu, S. K. (2025). Advancements in UAV remote sensing for agricultural yield estimation: A systematic comprehensive review of platforms, sensors, and data analytics. *Remote Sensing Applications: Society and Environment*, 37, 101418.

[5] Gao, K., Liu, B., Yu, X., Qin, J., Zhang, P., & Tan, X. (2020). Deep relation network for hyperspectral image few-shot classification. *Remote Sensing*, 12(6), 923.

[6] Joshi, P., Sandhu, K. S., Dhillon, G. S., Chen, J., & Bohara, K. (2024). Detection and monitoring wheat diseases using unmanned aerial vehicles (UAVs). *Computers and Electronics in Agriculture*, 224, 109158.

[7] Kachman, S., & Smith, J. (1995). Alternative measures of accuracy in plant spacing for planters using single seed metering. *Transactions of the ASAE*, 38(2), 379-387.

[8] Kamilaris, A., & Prenafeta-Boldú, F. X. (2018). Deep learning in agriculture: A survey. *Computers and Electronics in Agriculture*, 147, 70-90.

[9] Li, S. P., Zheng, C. R., Wen, C. M., et al. (2024). Localization Method for Missing Seedlings in Ratoon Sugarcane Based on UAV RGB Images and Improved YOLO v5s. *Transactions of the Chinese Society for Agricultural Machinery*, 55(12), 57-70.

[10] Liu, M., Su, W.-H., & Wang, X.-Q. (2023). Quantitative evaluation of maize emergence using UAV imagery and deep learning. *Remote Sensing*, 15(8), 1979.

[11] Liu, S., Qi, L., Qin, H., Shi, J., & Jia, J. (2018). Path aggregation network for instance segmentation. *Proceedings of the IEEE conference on computer vision and pattern recognition*, pp. 8759-8768, doi: 10.1109/CVPR.2018.00913.

[12] Liu, T., Li, R., Jin, X., Ding, J., Zhu, X., Sun, C., & Guo, W. (2017). Evaluation of seed emergence uniformity of mechanically sown wheat with UAV RGB imagery. *Remote Sensing*, 9(12), 1241.

[13] Pereyra, V. M., Bastos, L. M., de Borja Reis, A. F., Melchiori, R. J., Maltese, N. E., Appelhans, S. C., Vara Prasad, P., Wright, Y., Brokesh, E., & Sharda, A. (2022). Early-season plant-to-plant spatial uniformity can affect soybean yields. *Scientific Reports*, 12(1), 17128.

[14] Pham, M.-V., Ha, Y.-S., & Kim, Y.-T. (2023). Automatic detection and measurement of ground crack propagation using deep learning networks and an image processing technique. *Measurement*, 215, 112832.

[15] Ren, L., Li, C., Yang, G., Zhao, D., Zhang, C., Xu, B., Feng, H., Chen, Z., Lin, Z., & Yang, H. (2024). The Detection of Maize Seedling Quality from UAV Images Based on Deep Learning and Voronoi Diagram Algorithms. *Remote Sensing*, 16(19), 3548.

[16] Shirzadifar, A., Maharlooei, M., Bajwa, S. G., Oduor, P. G., & Nowatzki, J. F. (2020). Mapping crop stand count and planting uniformity using high resolution imagery in a maize crop. *Biosystems Engineering*, 200, 377-390.

[17] Singh, R., Singh, G., & Saraswat, D. (2005). Optimisation of design and operational parameters of a pneumatic seed metering device for planting cottonseeds. *Biosystems Engineering*, 92(4), 429-438.

[18] Sunoj, S., Igathinathane, C., Flores, J., Sidhu, H., Monono, E., Schatz, B., Archer, D., & Hendrickson, J. (2025). Crop row identification and plant cluster segmentation for stand count from UAS imagery based on profile and geometry. *Smart Agricultural Technology*, 11, 100938.

[19] Tetila, E. C., Moro, B. L., Astolfi, G., da Costa, A. B., Amorim, W. P., de Souza Belete, N. A., Pistori, H., & Barbedo, J. G. A. (2024). Real-time detection of weeds by species in soybean using UAV images. *Crop Protection*, 184, 106846.

[20] Tian, Y., Ye, Q., & Doermann, D. (2025). Yolov12: Attention-centric real-time object detectors. *arXiv preprint arXiv:2502*.12524.

[21] Valente, J., Sari, B., Kooistra, L., Kramer, H., & Mücher, S. (2020). Automated crop plant counting from very high-resolution aerial imagery. *Precision Agriculture*, 21(6), 1366-1384.

[22] Varela, S., Dhodda, P. R., Hsu, W. H., Prasad, P. V., Assefa, Y., Peralta, N. R., Griffin, T., Sharda, A., Ferguson, A., & Ciampitti, I. A. (2018). Early-season stand count determination in corn via integration of imagery from unmanned aerial systems (UAS) and supervised learning techniques. *Remote Sensing*, 10(2), 343.

[23] Vong, C. N., Conway, L. S., Feng, A., Zhou, J., Kitchen, N. R., & Sudduth, K. A. (2022). Corn emergence uniformity estimation and mapping using UAV imagery and deep learning. *Computers and Electronics in Agriculture*, 198, 107008.

[24] Zhang, X., Zeng, H., Guo, S., & Zhang, L. (2022). Efficient long-range attention network for image super-resolution. *European conference on computer vision*, 649-667.